Magn Reson Mater Phy (2010) 23:227–241
DOI 10.1007/s10334-010-0221-z

RESEARCH ARTICLE

^{1}H-MRS of brain metabolites in migraine without aura: absolute quantification using the phantom replacement technique

Harmen Reyngoudt · Yves De Deene · Benedicte Descamps · Koen Paemeleire · Eric Achten

Received: 12 April 2010 / Revised: 21 June 2010 / Accepted: 23 June 2010 / Published online: 13 August 2010

Abstract
Objective Several studies have demonstrated differences in migraine patients when performing ^{1}H-MRS; however, no studies have performed ^{1}H-MRS in migraine without aura (MwoA), the most common migraine subtype. The aim of this ^{1}H-MRS study was to elucidate whether any differences could be found between MwoA patients and controls by performing absolute quantification.
Materials and methods ^{1}H-MRS was performed in 22 MwoA patients and 25 control subjects. Absolute quantification was based on the phantom replacement technique. Corrections were made for T_1 and T_2 relaxation effects, CSF content, coil loading and temperature. The method was validated by phantom measurements and in vivo measurements in the occipital visual cortex.
Results After calibration of the quantification procedure and the implementation of the required correction factors, measured absolute concentrations in the visual cortex of MwoA patients showed no significant differences compared to controls, in contrast to relative results obtained in earlier studies.
Conclusion In this study, we demonstrate the implementation of quantitative in vivo ^{1}H-MRS spectroscopy in migraine patients. Despite rigorous quantification, no spectroscopic abnormalities could be found in patients with migraine without aura.

Keywords Absolute quantification · ^{1}H-MRS · migraine without aura · correction factors · phantom replacement technique

H. Reyngoudt · B. Descamps · E. Achten (✉)
Department of Radiology and Nuclear Medicine,
Ghent Institute for Functional and Metabolic Imaging,
Ghent University, Ghent, Belgium
e-mail: rik.achten@ugent.be

H. Reyngoudt · B. Descamps · E. Achten
MR-department, Ghent University Hospital,
De Pintelaan 185, 9000 Ghent, Belgium

H. Reyngoudt
e-mail: harmen.reyngoudt@ugent.be

Y. De Deene
Department of Radiation Oncology and Experimental Cancer Research, Laboratory for Quantitative Nuclear Magnetic Resonance in Medicine and Biology,
Ghent University, Ghent, Belgium

Y. De Deene
Department of Nuclear Medicine and Radiobiology,
University of Sherbrooke, Sherbrooke, Quebec, Canada

K. Paemeleire
Department of Basic Medical Sciences,
Ghent University, Ghent, Belgium

K. Paemeleire
Department of Neurology, Ghent University Hospital,
Ghent, Belgium

Introduction

Migraine is a common, chronic, disabling neurovascular disorder, with episodic manifestations, characterized by attacks of headache lasting 4–72 h, and associated symptoms such as photophobia, phonophobia, nausea and/or vomiting [1–4]. In 20–30% of the patients, aura symptoms are experienced [1,2]. Migraine has a 1-year prevalence of at least 11% worldwide [5], affects women three times more than men [5] and has a high socio-economic impact [6]. It has been ranked nineteenth as worldwide cause of years lived with disability, according to the World Health Organization [7]. Migraine is a primary headache disorder, with an important genetic background and can be divided into two major subtypes: migraine

Table 1 Literature survey of ^{1}H-MRS studies in migraine (*n* is the number of patients included)

Study	Magraine type (*n*)	Brain region	Quantification	Results
Watanabe et al. [19]	MwA/other[a] (3/3)	Occipital	Relative	Lac/NAA ↑
Macri et al. [26]	MwA (8)	Cerebellum	Relative	Ins/tCr ↓, Cho/tCr ↓
Sandor et al. [20][b]	MwA/MwpA (5/5)	Occipital	Relative	Lac/NAA ↑
Dichgans et al. [22]	FHM[d] (15)	Cerebellum	Absolute	Glu ↓, NAA ↓, Ins ↑
Sarchielli et al. [21][c]	MwA/MwoA (22/22)	Occipital	Relative	NAA/tCr ↓
Jacob et al. [23]	SHM[e] (1)	Temporo-parietal	Relative	NAA/tCr ↓, Ins/tCr ↓
Schulz et al. [24]	MwA (21)	Basal ganglia	Relative	No changes
Gu et al. [25]	MwoA (22)	Thalamus	Relative	NAA/tCr ↓
Grimaldi et al. [28]	FHM (4)	Parieto-occipital	Relative	Lac ↑

[a] Basilar migraine, migrainous infarction and MwpA
[b] Visual stimulation was performed by projection of a blue/yellow flickering checkerboard (8 Hz)
[c] Familial hemiplegic migraine
[d] Visual stimulation was performed by projection of a flashing red light (14 Hz)
[e] Sporadic hemiplegic migraine

without aura (MwoA) and migraine with aura (MwA), previously known as common and classic migraine, respectively [4]. Despite the high prevalence of migraine in the general population, the causes are still unknown. One hypothesis is that migraine is a disorder that might be caused by the concurrence of two pathophysiological components: excessive cortical activation due to lack of habituation during repetitive stimulation as well as a decreased brain mitochondrial energy reserve [8,9].

In the last 20 years several magnetic resonance spectroscopy (MRS) studies, in particular phosphorus magnetic resonance spectroscopy (^{31}P-MRS), suggested an energy disturbance in the brain of migraine patients during interictal periods [10–18]. Recent studies emphasized more on proton magnetic resonance spectroscopy (^{1}H-MRS) with a lot of heterogenous, sometimes contradictory, results (Table 1). ^{1}H-MRS studies showed elevated interictal levels of cerebral lactate (Lac) in the occipital visual cortex of a heterogeneous group of migraine patients [19]. These results suggested a deranged oxidative glycolysis. In functional ^{1}H-MRS studies, visual stimulation resulted in a Lac increase in the visual cortex of patients with migraine with prolonged aura (MwpA) but not in MwA patients, in which Lac was already higher than normal [20] and N-acetylaspartate (NAA) was found to be reduced in the visual cortex of MwA patients [21]. A reduced NAA concentration was also found in several other brain regions of MwA patients without stimulation [22,23,25]. In other than occipital regions, significant differences for other metabolites such as myo-inositol (Ins), total creatine (tCr), choline (Cho) and glutamate/glutamine (Glx) have been found between migraineurs and controls [22,23,26,27].

Very few studies have quantified proton metabolites in the subgroup of MwoA patients. From these studies in which ^{1}H-MRS was performed, only relative quantification was applied and/or spectra were acquired following visual stimulation (Table 1). From this point of view, we took a great interest in verifying whether there was indeed a basal interictal metabolic deficiency in the occipital visual cortex of these migraine patients. In order to confirm if there are subtle differences compared to controls, robust absolute quantification of these metabolites is necessary. In this study, we first describe the rigorous methodological setup of absolute quantification of metabolites in the visual cortex using ^{1}H-MRS, based on the phantom replacement technique. Important methodological parameters of absolute quantification were considered and taken into account, including reproducibility, stability, B_0 homogeneity, B_1 homogeneity, relaxation effect correction, temperature correction and cerebrospinal fluid content correction. Absolute quantification using the internal water reference was also performed. The optimized method was then applied to address the question of interictal metabolite abnormalities in the occipital visual cortex of MwoA patients when compared to normal controls.

Materials and methods

Acquisition, voxel placement, subjects and phantoms

Measurements were taken on a 3 Tesla Siemens Trio-Tim whole-body MR scanner (Erlangen, Germany), using a 26.5-cm-diameter quadrature dual-tuned (^{31}P-^{1}H) birdcage transmit/receive head coil (Rapid Biomedical, Würzberg-Rimpar, Germany). Spectra were acquired using a single voxel point–resolved spin echo sequence (PRESS), with CHESS pulses for water suppression. Manual shimming of the B_0 magnetic field and manual optimization of the transmitter pulse power was applied. Twenty-two MwoA patients (33.3 ± 12.2 years, 1 man) were recruited by the local Headache Clinic of the Ghent University Hospital. The control

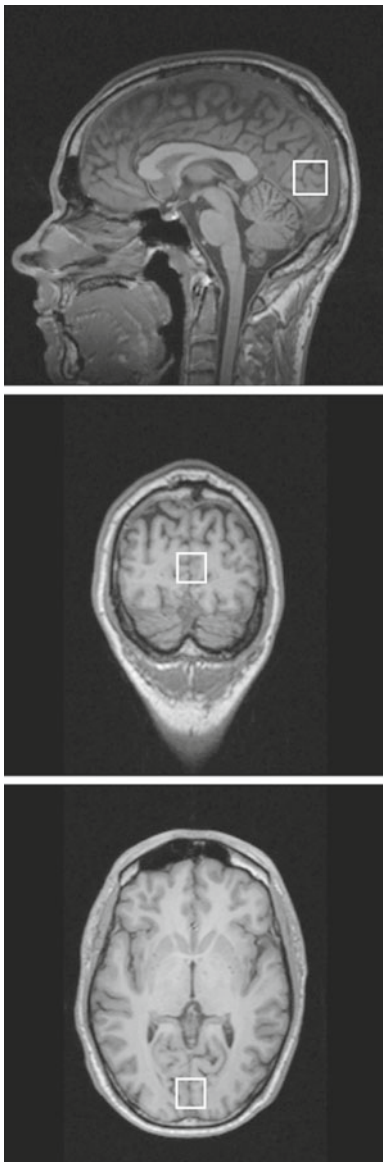

Fig. 1 Sagittal, coronal and axial T_1-weighted images with a 20 mm cubic VOI localized in the occipital visual cortex

group (27.6 ± 12 years, 10 men) consisted of twenty-five volunteers which were matched in age but not in gender. All subjects have given written consent, and the study was approved by the local ethics committee. The migraine patients were diagnosed with MwoA according to the criteria of the International Headache Society [4]. On average, patients experienced 3.4 ± 1.1 attacks per month, were not using any prophylactic medication and were attack free for at least 48 h. A possible attack after the measurement was verified by e-mail.

The volume of interest (VOI) was placed in the primary visual cortex (Brodmann area 17), centered on the calcarine fissure (Fig. 1), localized on T_1-weighted gradient-echo images in three orthogonal planes with a slice thickness of 1 mm, a TR of 1,550 ms and a TE of 2.37 ms. VOI size was $20 \times 20 \times 20\,\text{mm}^3$. For each subject, six water-suppressed spectra at different TE (30, 60, 90, 120, 144 and 288 ms) with a TR of 4,000 ms and 64 averages, one water-suppressed spectrum with a TE of 30 ms, a TR of 2,000 ms and 96 averages and ten water-unsuppressed spectra (TE = 30, 50, 70, 90, 110, 150, 200, 300, 500, 1000 ms, TR = 10,000 ms, 1 average) were acquired. The raw data of each acquisition consisted of 1,024 complex-valued data points, at a sampling interval of 0.833 ms. The corresponding bandwidth was 1,200 Hz. The total duration of the examination was approximately 50 min.

The phantoms contained an aqueous solution (pH 7) of NAA, tCr, Cho and Ins (Sigma Aldrich) in different concentrations and combinations. Sodium chloride (NaCl) and sodium azide (NaN_3) were added to change the conductivity and as an antimycotic agent, respectively. Phantoms were made of plastic, were spherical and had a diameter of 10.4 cm. One of the phantoms consisted of an aqueous solution of 12 mM NAA, 10 mM tCr, 3 mM Cho and 6 mM Ins, to which 1% NaCl was added to simulate the physiological NaCl concentration, referred to further as the standard metabolite solution.

Spectral analysis

Water-unsuppressed spectra were processed without apodization and fitted by a single component using HLSVD, a method based on the Lanczos algorithm and included in the jMRUI package [29], yielding an estimation of the water signal amplitude. The residual water resonance was removed by HLSVD [30]. The signals of Lac, NAA, tCr and Cho were referenced at 1.31, 2.01, 3.03 and 3.19 ppm, respectively. The strongly coupled signal of Ins is referenced at 3.55 and 3.61 (Fig. 2). Following apodization (Lorentzian filter of 5 Hz), zero-filling (adding 1,024 zeros) and baseline correction, the water-suppressed spectra were fitted by the time-domain algorithm AMARES [31,32], software that is also included in the jMRUI package. This nonlinear least-squares algorithm fits a time-domain model function, using a singlet approach at a priori predefined resonance frequencies. The AMARES algorithm also includes other prior knowledge such as lower and upper bounds of the spectral parameters (frequency, linewidth, phase), Gaussian instead of Lorentzian lineshape for each peak and modulation of the background signal. In this study, Gaussian lineshapes and a least-squares fit were used in order to avoid problems from occasional minimal overlap of Cho and tCr peaks (Fig. 2c). Quantification of short TE in vivo signals is often hampered by a background signal originating mainly from macromolecules and lipids (Fig. 2b). In order to minimize the signals of macromolecules and lipids of water-suppressed spectra, AMARES gives the opportunity to truncate the initial data points [31].

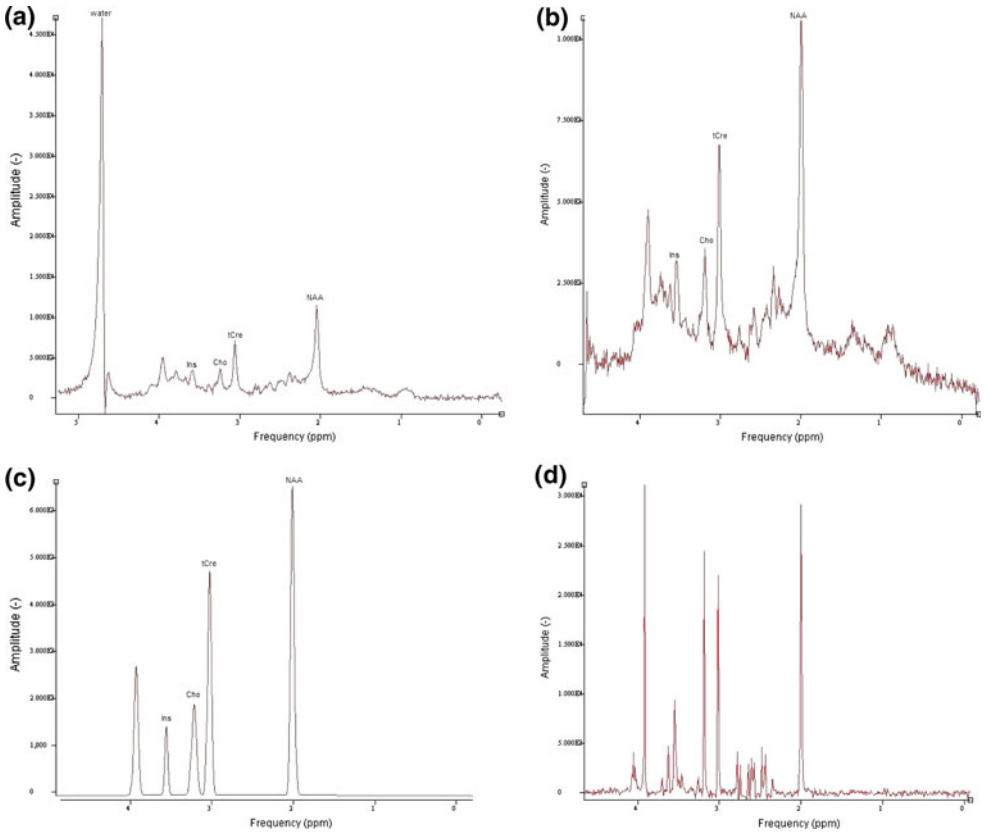

Fig. 2 Spectrum obtained in a patient with a water-suppressed PRESS sequence with a TE of 30 ms, a TR of 2,000 ms and 128 averages before (**a**) and after (**b**) removal of the residual water resonance. Notice the significant background signal in the in vivo spectra. **c** An estimation of the in vivo metabolites based on spectrum **b** with removal of the macromolecular background signal by AMARES. **d** Spectrum obtained in a 20 mm cubic VOI in a phantom containing 12 mM NAA, 10 mM tCr, 3 mM Cho and 6 mM Ins

We truncated the first 20 data points, in order not to influence the quantification of the metabolites.

Reproducibility and stability

Before using the phantom for calibration of the in vivo signals, the influence of several scanning factors on signal amplitude, such as reproducibility and stability of the signal, was investigated.

Stability of the scanner, repeatability and reproducibility of the measurements were verified in both phantom and in vivo experimental setups. Repeatability and reproducibility both refer to the precision of the measurement and the ability to repeat and reproduce the experiment. In this study, repeatability is interpreted as consecutive measurements without repositioning and reshimming of the phantom, and reproducibility is interpreted as measurements with repositioning and reshimming of the phantom. In the phantom containing the standard metabolite solution, fifteen measurements were taken in the same voxel (VOI $= 20 \times 20 \times 20\,\text{mm}^3$) without repositioning and reshimming, followed by five additional measurements each time with repositioning and reshimming of the phantom. The VOI was placed in the center of the phantom. This experiment was also repeated after one week, one month, six months and one year. In ten controls, two consecutive measurements were taken in the same voxel (VOI $= 20 \times 20 \times 20\,\text{mm}^3$) without repositioning and reshimming. Finally, we verified the in vivo reproducibility by repeating the experiment 16 times during one year in a single healthy volunteer (male, 29 years).

B_0 homogeneity

When a phantom or a subject is scanned, the magnetized object or body distorts the net magnetic field. Especially in heterogenous media, composed of tissue with different magnetic susceptibilities, significant errors may be induced in the spectra [33]. Local B_0 inhomogeneities widen and distort the spectral lines from the ideal Lorentzian form [34]. The homogeneity of the B_0 field can be optimized by automatic and manual shimming. Manual shimming was performed until the linewidth or full-width-at-half-maximum (FWHM) was equal to or lower than 0.1 ppm or 12 Hz for $B_0 = 3$ T and the time-domain signal showed an exponential decay [33,35].

We verified the effect of incomplete shimming in a phantom containing an aqueous solution of 20 mM tCr (1% NaCl, pH 7). A first measurement was taken with optimized shim settings, followed by several other measurements with intentionally insufficient shimming (i.e. inhomogeneous B_0 field). The FWHM of the spectral peaks of all metabolites and water were verified in every volunteer.

B_1 homogeneity

It is assumed that in spectral quantification based on the phantom replacement technique, spatial sensitivity remains the same for the phantom and the in vivo measurement. In practice, there may be unexpected variations in signal intensity due to B_1 inhomogeneity, effects related to loading, eddy currents and standing waves [36]. These variations may depend on the size of the phantom, the electrical properties of the phantom and the corresponding properties of the human head. The spatial distribution of the B_1 field was investigated by the double-angle method, which measures the flip angle distribution within the sample [37]. This is an indirect measure of the B_1 field and can reveal standing waves in the coil. Two gradient-echo images, I_1 and I_2, with corresponding flip angles θ and 2θ were recorded. The flip angle distribution is given by:

$$\theta = Arccos\left(\frac{I_2}{I_1}\right). \quad (1)$$

These images were obtained in two water-filled phantoms by a gradient-echo pulse sequence with a TE of 4.15 ms, a TR of 10,000 ms, slice thickness of 5 mm and a nominal θ of 35°. The two phantoms contained a 0 and 1% NaCl solution, respectively.

We further evaluated the potential presence of standing waves by positioning the voxel in different locations (central and off-center) in phantoms with different NaCl concentration (0, 0.5, 1, 1.5 and 2%) in order to change the dielectric properties of the phantom.

The effect of coil-related inhomogeneity was investigated by placing a water-filled phantom with 20 mm cubic VOIs at the system isocenter and at offsets of ±30, ±60 and ±90 mm along the *x*-, *y*- and *z*-axes. Spectra were acquired with the phantom repositioned between each acquisition with the VOI always located in the center of the phantom. A single-shot acquisition was used, with a TE of 30 ms, a TR of 10,000 ms and no water suppression. Each measurement was taken with separate optimization of the transmitter pulse voltage (V_{tra}).

Absolute quantification

The complete equation for calculating the absolute in vivo concentrations, using the phantom replacement technique, is given by [33]:

$$[C_i] = [C_r]\frac{S_i V_r N_r c_{T1r} c_{T2r} T_i \rho_i c_{\text{load}}}{S_r V_i N_i c_{T1i} c_{T2i} T_r \rho_r c_{\text{csf}}} \quad (2)$$

where subscripts i and r correspond with in vivo and the reference phantom, respectively, $[C]$ is the metabolite concentration, the tCr metabolite concentration $[C_r]$ in the reference phantom was 10 mM, S is the signal strength, V is the volume of the voxel from which the signal is acquired, N is the number of protons that contribute to the spectral line ($N = 3$ for NAA and tCr, $N = 9$ for Cho and $N = 2$ for Ins and water), c_{T1} and c_{T2} are correction factors for the signal loss caused by T_1 and T_2, respectively, T is the absolute temperature ($T_i = 37$°C in the human subject and $T_r = 21$°C in the reference phantom), ρ is the density of water, c_{load} is a correction factor that accounts for different coil loading (i.e. the respective V_{tra}s) and c_{csf} is the correction factor for partial volume effects (i.e. the fraction of CSF compared to the fraction of water in the brain parenchyma in the VOI). The volume ratio V_r/V_i cancels from the equation since V was the same in the reference phantom and in vivo, i.e. $20 \times 20 \times 20\,\text{mm}^3$.

When using the internal water reference for absolute quantification, the equation has to be adjusted for the reference concentration, being 55 M [38], and for T_1 and T_2 of water. The corrections for temperature and coil loading cancel from the equation, when the internal water signal is used as a reference.

Relaxation times

The acquired signal must be corrected for T_1 and T_2 decay as the measurement was performed with a TE of 30 ms and a TR of 2,000 ms, corresponding with a considerable loss of signal in the transverse plane and a not fully relaxed signal in the longitudinal direction, respectively. The relaxation decay times were determined in the phantom and in vivo. The phantom containing the standard metabolite solution was used. For the phantom measurement T_1 relaxation times, a water-suppressed PRESS sequence was used with thirty different repetition times (between 1,120 and 30,000 ms), a TE of 30 ms and 128 averages. For the measurement of the phantom T_2 relaxation times, a water-suppressed PRESS sequence was used with twenty-four different echo times (between 30 and 1,500 ms), a TR of 10,000 ms and 128 averages.

The determination of T_2 was performed in all volunteers (MwoA patients and controls) with the same water-suppressed PRESS sequence with six different echo times (TE = 30, 60, 90, 120, 144 and 288 ms), a TR of 4,000 ms and 64 averages. In order not to expose the MwoA patients and the controls to excessive scan times, the measurement of in vivo T_1 relaxation times was performed in an additional group of age- and gender-matched healthy volunteers ($n = 12$,

men/women = 5/7, age = 28.5 ± 4.8 years). The same water-suppressed PRESS sequence was used with eight different repetition times (TR = 1,500, 2,000, 2,500, 3,000, 3,500, 4,000, 6,000 and 10,000 ms), a TE of 30 ms and 64 averages. T_1 and T_2 relaxation times were calculated by fitting the peak areas determined by AMARES, to single-exponential functions, using a Levenberg-Marquardt algorithm in MATLAB (Mathworks, Natick, MA):

$$S = S_0\, e^{-TE/T_2} \tag{3}$$

$$S = S_0\,(1 - e^{-TR/T_1}) \tag{4}$$

The correction factors are given by:

$$c_{T2} = e^{-TE/T_2} \tag{5}$$

$$c_{T1} = (1 - e^{-TR/T_1}) \tag{6}$$

Temperature

Temperature has to be taken into account as it has an influence on the spin populations, according to the Boltzmann distribution. A 5 % difference between the in vivo signal (i.e. body temperature) and the reference signal (i.e. room temperature) is found [33,39]. Temperature has also an influence on the water density; however, in the temperature range from 20 to 37°C, this influence is negligible. Temperature in the phantoms was verified regularly.

Coil loading

When applying the phantom replacement technique for absolute quantification, a correction is needed to compensate for the change in coil loading between volunteer and the phantom [40–42]. The change in coil loading is related to the difference in electrical conductivity and shape of the scanned subject or phantom [33]. The correction method is based on the principle of reciprocity, which states that (for combined transmit/receive coils) the external voltage needed to produce a certain B_1 at a given location is inversely proportional to the voltage induced by a predefined B_1 [43]. A measure of the local B_1 in a certain VOI can be derived from the V_{tra} required to obtain a 90° excitation pulse. According to the principle of reciprocity, the product of the received signal and V_{tra} is constant, under varying loading conditions [33]. This was verified by measuring a set of phantoms containing an aqueous solution of 10 mM tCr with varying NaCl concentration (0, 0.5, 1, 1.5 and 2%), simulating differential coil loading. The correction factor c_{load} used in Eq. 2 is calculated by the following correction factor:

$$c_{load} = \frac{V_{tra,in\ vivo}}{V_{tra,phantom}} \tag{7}$$

where $V_{tra,in\ vivo}$ and $V_{tra,phantom}$ are the transmitter voltages, determined in vivo and in the reference phantom, respectively.

Partial volume effects

Brain tissue consists of different compartments (gray matter, white matter, CSF, blood), and this compartmentalization is spatially dependent [44]. Metabolite concentrations are often underestimated when the contribution of cerebrospinal fluid is not accounted for [45]. There are several segmentation approaches, all of which are based on differences in relaxation properties. Next to image segmentation [46], the determination of the CSF compartment can also be accomplished by a series of spectra in which the signal amplitude of water is measured as a function of TE, yielding T_2 [42,47]. Based on the differences in T_2 between CSF and brain tissue water, the CSF contribution can be easily determined [40,44]. The double-exponential decay of the water signal was measured using a single shot water-unsuppressed PRESS sequence with ten different echo times (TE = 30, 50, 70, 90, 110, 150, 200, 300, 500 and 1,000 ms) and a TR of 10,000 ms. The signal amplitudes of CSF and brain tissue water were extracted using a Levenberg–Marquardt algorithm in MATLAB, using the following equation:

$$\begin{aligned} S = {} & S_{0,csf}\, e^{-TE/T_{2,csf}}(1 - e^{-TR/T_{1,csf}}) \\ & + S_{0,bw}\, e^{-TE/T_{2,bw}}(1 - e^{-TR/T_{1,bw}}) \end{aligned} \tag{8}$$

with $T_{1,csf}$, $T_{2,csf}$, $T_{1,bw}$ and $T_{2,bw}$ the longitudinal and transverse relaxation times of CSF and brain water (bw), respectively and $S_{0,csf}$ and $S_{0,bw}$ the unrelaxed signal amplitudes of CSF and brain water, respectively. The signal intensity with the longer T_2 was assigned to CSF. The correction factor c_{csf} used in equation 2 is determined by the following ratio:

$$c_{csf} = 1 - \frac{S_{0,csf}}{S_{0,bw} + S_{0,csf}} \tag{9}$$

Statistical analysis

Statistical analysis was performed using the SPSS software (SPSS 15.0 for Windows, Chicago, IL). Descriptive statistics were calculated for age, sex, T_1, T_2, V_{tra}, c_{csf}, absolute metabolite concentrations and metabolite ratios. The *t*-test for unpaired data was applied. Analyses were done on T_1, T_2, V_{tra}, c_{csf}, absolute metabolite concentrations and metabolite ratios between MwoA patients and controls, and between men and women. Results were considered to be significant at $P < 0.05$. For V_{tra} and c_{csf}, a nonparametric test for unpaired data (Mann–Whitney *U*-test) was applied. Coefficients of variation (CV), defined as the ratio of standard deviation and mean (in %), were calculated for repeatability, reproducibility, B_0 homogeneity, the inter-subject variation of T_1 and T_2

Table 2 Repeatability, reproducibility and signal amplitudes: CV (%)

	NAA	tCr	Cho	Ins
15 Consecutive measurements in 1 phantom	1.83	1.44	1.53	3.23
30 Measuremtents spread over 1 year in 1 phantom	4.62	4.01	5.63	12.45
2 Consecutive measurements in 10 healthy subjects	1.99	3.59	8.23	5.58
18 Measurements spread over 1 year in 1 healthy subject	3.42	4.65	11.99	8.56

relaxation times and the errors on the absolute metabolite concentrations.

Results

Reproducibility and stability

Accuracy of the single voxel spectroscopy measurement can be verified by both repeatability and reproducibility (Table 2). When performing consecutive measurements (= repeatability) in the same voxel without repositioning the phantom, the V_{tra}-value had a CV of 0.16%. Variation of the metabolite signals, corrected for coil loading, ranged from 1.44% for tCr to 3.23% for Ins. Variation of these metabolite signals, again corrected for coil loading, measured within the same phantom at several times spread over a timespan of a year (= reproducibility), ranged from 4.62% for NAA to 12.45% for Ins. V_{tra} had a CV of 1.33% (Table 2; Fig. 3a).

The average CV of the metabolite signals when performing consecutive measurements in ten healthy subjects ranged from 1.99% for NAA to 8.23% for Cho. Finally, the CV of the metabolite signals when performing measurements on regular time points during the year in one healthy subject ranged from 3.42% for NAA to 11.99% for Cho (Table 2; Fig. 3b).

B_0 homogeneity

Upon shimming, a spectral width of 3–5 Hz could easily be achieved for the water resonance in phantoms. When deliberately increasing the FWHM of the water resonance in increments of 5 Hz to about 35 Hz, we observed a CV of 12.86 ± 6.39 % for the tCr signal in a phantom, when comparing to the optimally shimmed water resonance of 5 Hz. In vivo we achieved on average a spectral width of 15.42 ± 1.48 Hz for water in the occipital visual cortex. The FWHM for the main metabolites in vivo ranged from 8.34 ± 1.80 Hz for NAA to 10.87 ± 3.13 Hz for Cho.

B_1 homogeneity

Figure 4 shows the signal intensity profiles of the water resonance, obtained in a small spherical phantom. Spatial variation has been calculated from signal intensities measured

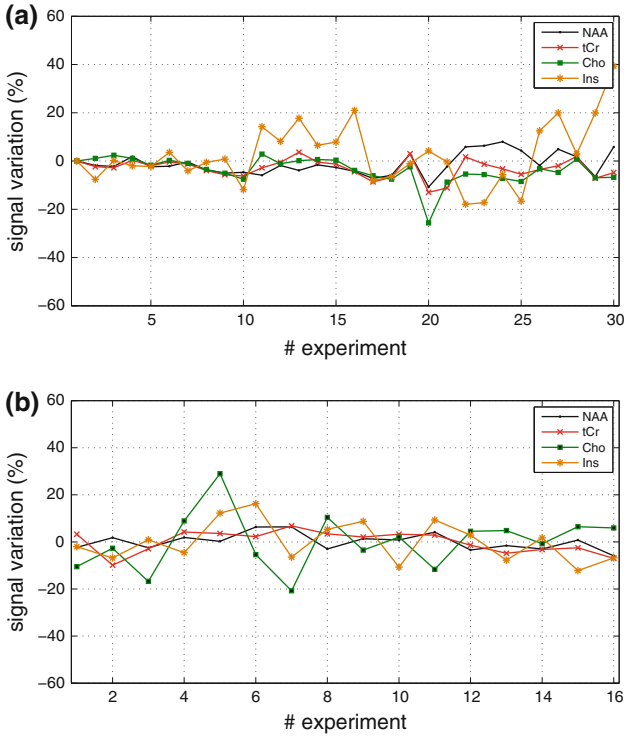

Fig. 3 **a** Signal variation in a phantom measured at different time points during the year (with the value of the first measured time point normalized to 0%). **b** Signal variation in one subject measured at different time points during the year (with the average value normalized to 0%). Experiments are shown chronologically

within 20 mm cubic VOIs with offsets along all three Cartesian axes of up to 90 mm. Signal intensity is defined to be 0% at the isocenter, so significant deviation of mean signal intensities from this value indicates variation in response along one or more axes. Different spatial variations were observed along different axes (as shown in Fig. 4). A signal intensity variation of 5.40, 3.04 and 4.97% was observed in the z-, y- and x-directions, respectively.

The variation in signal intensity was quite similar in all phantoms with different NaCl concentrations with the highest variation closest to the edge of the phantoms (Fig. 5). The smallest variation (2.76%) was found in the 1%-NaCl-doped phantom. Figure 6 shows the flip angle images in the axial plane obtained in the phantoms containing 0 and 1% NaCl. The mean flip angle and the corresponding standard deviation

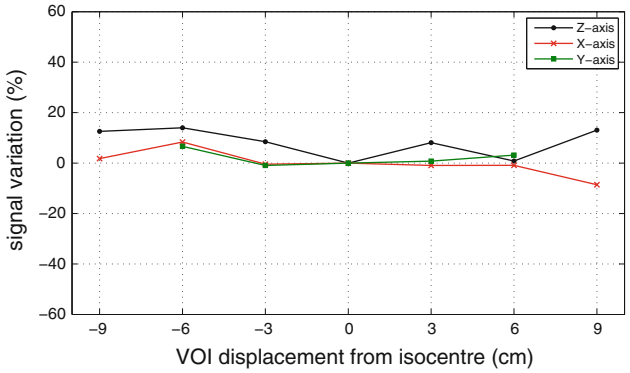

Fig. 4 Spatial variation in the water signal intensity with respect to the value at the isocenter (normalized to 0% at the isocenter) in a small water-filled phantom. The excitation pulse flip angle was optimized at each VOI location

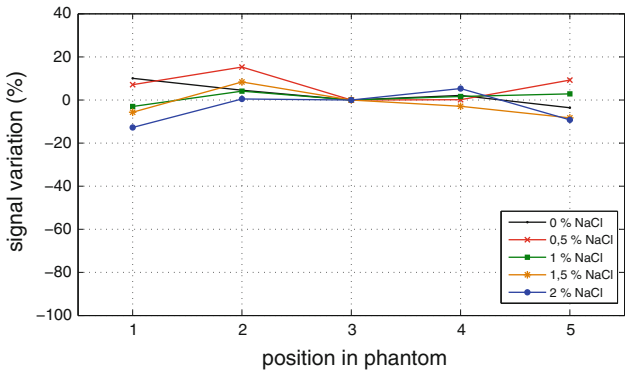

Fig. 5 Spatial variation in signal intensity for different NaCl concentrations (normalized to 0% at the central position in the phantom), with optimization of the excitation pulse flip angle at isocenter at each VOI. Positions 1 and 5 are VOIs closest to the edge of the phantom

were 32.87 ± 2.21 ° and 37.74 ± 2.34 °, respectively. As can be seen, there are no significant deviations from the nominal flip angle in both phantoms.

Relaxation times

Relaxation times of the metabolites, both in the phantom and in vivo, are listed in Table 3. The tCr signal was used as the external reference standard for absolute quantification of the in vivo metabolites. T_1 and T_2 relaxation times of brain water and CSF are listed separately in Table 3 and were also derived from the double-exponential fit of the water decay. There were no significant differences in relaxation times between MwoA patients and controls ($P \geq 0.113$), nor between men and women ($P \geq 0.100$). The T_2-value of Ins could not be determined since the signal of Ins does not follow a single- or double-exponential with multiple echo times.

Table 3 Relaxation times

	T_1 (ms, ±SD)	T_2 (ms, ±SD)
Phantom[a]		
H_2O	2,860 ± 177	2,275 ± 77
NAA	1,267 ± 84	1,247 ± 84
tCr	1,825 ± 95	1,385 ± 108
Cho	1,934 ± 76	1,882 ± 101
Ins	1,117 ± 51	–
In vivo		
H_2O (CSF)	2,897 ± 701[b]	670 ± 120[b]
H_2O (bw)	484 ± 113[b]	70 ± 6[b]
NAA	1,448 ± 99[c]	224 ± 27[b]
tCr	1,424 ± 146[c]	146 ± 23[b]
Cho	1,380 ± 232[c]	148 ± 38[b]
Ins	1,113 ± 201[c]	–

[a] All values were the average of six identical measurements
[b] These values were the average 22 MwoA patients and 25 controls
[c] These values were the average of an additional group of 12 controls

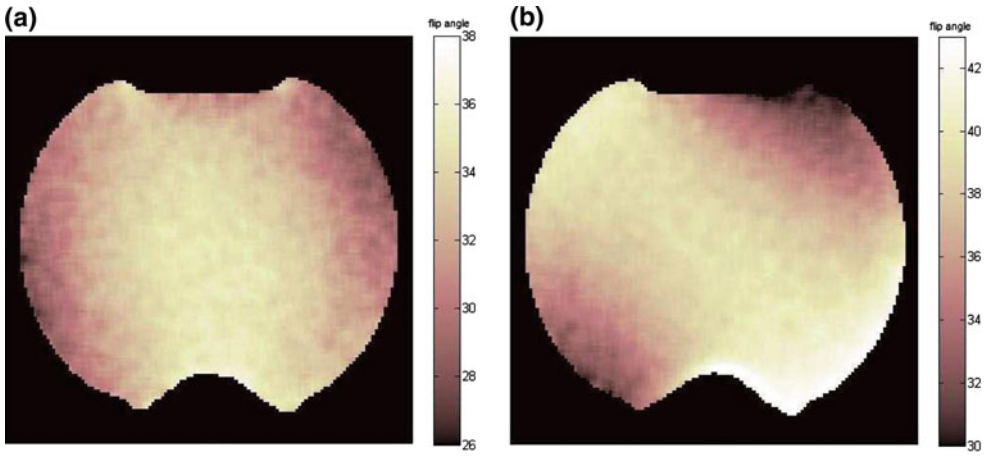

Fig. 6 Axial flip angle images for phantoms containing 0 % (**a**) and 1% NaCl (**b**), respectively. The nominal flip angle (θ) was 35°

Temperature

No significant temperature variations were observed over the phantom measurements during the study. Temperature was always $20 \pm 0.7°C$.

Coil loading

The effect of different coil loading on the acquired signal in a phantom is demonstrated in Fig. 7. Signal amplitudes decrease with increasing NaCl concentration (and hence increased coil loading). Since V_{tra} is a direct measure of coil loading, Fig. 7 also illustrates an increase of V_{tra} with increasing NaCl concentration.

V_{tra} was 168.03 ± 8.06 V and 176.88 ± 12.86 V for MwoA patients and controls ($P = 0.001$), respectively. Whereas the V_{tra} in vivo was on average 170 V, the V_{tra}-value was 138.5 V when scanning the phantom.

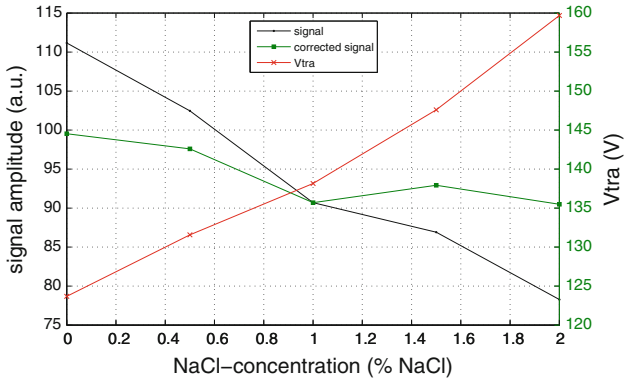

Fig. 7 Relation between the signal intensity (before and after correction), NaCl concentration and the V_{tra}

Partial volume effects

The CSF content is on average $11.84 \pm 4.17\%$. The CSF fraction does not show any significant differences both between MwoA patients ($12.00 \pm 4.70\%$) and controls ($12.58 \pm 4.10\%$) and between men ($13.00 \pm 4.36\%$) and women ($12.00 \pm 4.38\%$), respectively. The P-values were 0.719 and 0.927, respectively.

Absolute quantification

The quantification protocol was evaluated using a phantom containing an aqueous solution of 15 mM NAA (pH 7) and 2% NaCl to simulate a different coil loading. The phantom containing the standard metabolite solution was used as a reference. After taking into account correction factors for T_1, T_2 and coil loading, the absolute concentration of NAA was found to be 15.22 mM NAA, which results in an error of 1.01%. There was no temperature difference between these phantoms.

Table 4 shows the absolute concentrations of NAA, tCr, Cho and Ins, with their corresponding standard deviations, in the occipital visual cortex of 22 MwoA patients and 25 controls. These values were obtained after applying corrections for T_1, T_2 (except for Ins in vivo), coil loading, temperature and CSF, as described above. Absolute metabolite concentrations based on the internal water reference method and metabolite ratios are also listed in Table 4. For all concentrations and ratios, there were no significant differences between MwoA patients and controls ($P \geq 0.550$, Table 4). In addition, because the study population was age- but not gender-matched, a similar analysis was performed to compare male and female volunteers. This showed no significant differences in metabolite concentrations between men and women in the occipital visual cortex ($P \geq 0.100$).

Table 4 Absolute concentration values in mmol/(kg wet weight) and metabolite ratios (mean ±SD)[a]

	MwoA patients	Controls	Absolute quantification method
[NAA] (mmol/(kg ww))	11.39 ± 1.55	11.39 ± 1.35	Phantom replacement technique
	12.21 ± 1.78	11.56 ± 1.66	Internal water reference
[tCr] (mmol/(kg ww))	8.78 ± 1.59	8.96 ± 1.37	Phantom replacement technique
	9.37 ± 1.53	9.03 ± 1.46	Internal water reference
[Cho] (mmol/(kg ww))	1.59 ± 0.41	1.58 ± 0.47	Phantom replacement technique
	1.70 ± 0.43	1.62 ± 0.43	Internal water reference
[Ins] (mmol/(kg ww))	2.44 ± 0.46	2.46 ± 0.65	Phantom replacement technique
	2.63 ± 0.58	2.52 ± 0.64	Internal water reference
NAA/tCr	1.44 ± 0.13	1.42 ± 0.18	–
Cho/tCr	0.18 ± 0.03	0.18 ± 0.05	–
Ins/tCr	0.38 ± 0.06	0.38 ± 0.09	–
Cho/NAA	0.12 ± 0.02	0.12 ± 0.03	–
Ins/NAA	0.27 ± 0.03	0.27 ± 0.05	–

[a] Significance level: $P < 0.05$

Discussion

In migraine, several magnetic resonance spectroscopy studies, in particular ^{31}P-MRS and a few ^{1}H-MRS studies, have been performed. Most of these studies suggested a metabolic disturbance in the brain of MwA patients and, to a lesser extent, of MwoA patients, which is evident even in the interictal period [10–18].

In MwoA, ^{1}H-MRS has only been performed following visual stimulation and using relative quantification. As already mentioned, only a few number of studies emphasized on MwoA. Only one study reports measurements from the occipital visual cortex. Sarchielli et al. observed no changes in the occipital cortex between MwoA patients and controls before visual stimulation; however, following stimulation, the NAA signal amplitude was found to be downregulated (unsignificantly) [21].

One other study (Gu et al.) found a significant decrease in NAA/tCr in the left thalamus of MwoA patients compared to controls [25].

Several other studies also performed ^{1}H-MRS in the occipital cortex, however, in other migraine subgroups. Sarchielli et al. found a significantly decreased NAA signal amplitude in MwA patients, both before and after visual stimulation [21]. Lactate was found increased in MwA and MwpA patients in several other studies [19–21]. In a few other studies, significant changes have been observed in other brain regions of MwA patients.

Because of the lack of quantitative ^{1}H-MRS data in MwoA patients and the assumption of a possible deficiency in the energy metabolism of the brain in these patients, in which tCr plays a vital role, a firm interest grew to perform absolute quantification with ^{1}H-MRS in this migraine subgroup.

In this study, we searched for possible interictal differences in metabolic concentrations in the occipital visual cortex between healthy subjects and MwoA patients by use of quantitative absolute ^{1}H-MRS. The assumption of a constant in vivo water concentration of 55 mM, as used with internal water referencing, was an important reason to prefer the phantom replacement technique for obtaining absolute concentrations [38]. To utilize a robust methodological ^{1}H-MRS protocol in this migraine study, several scanner properties such as reproducibility, B_0 and B_1 homogeneity were assessed in both phantom and in vivo situations. Absolute quantification also involves the determination of several correction factors such as relaxation times, coil loading effects and temperature. One of the big advantages of absolute quantification when compared to relative quantification is that it does not assume a constant metabolite concentration (e.g. tCr). Indeed, several studies have shown significant changes in both tCr and Cho [48,49]. In addition, if patients have global metabolic defects, comparisons with contralateral brain regions (which are assumed to be metabolically normal) are not possible [50,51]. To our knowledge, this was the first study in which absolute quantification was applied with ^{1}H-MRS in MwoA and migraine in general.

Quality assessment

When performing consecutive measurements in the same voxel of a phantom, without repositioning and reshimming, CVs were small for all metabolites (around 3% maximal). When repeating this experiment but now with repositioning and reshimming of the phantom, the CV increased for all metabolites and for V_{tra}. The reproducibility was also assessed by repeating the experiment after one week, one month, six months and one year, each time with repositioning and reshimming of the phantom. The CV for all metabolites during this period amounted to around 4 or 5% for NAA, tCr and Cho and 12.45% for Ins. V_{tra} had a CV of 1.33% during a 1-year period. No systematic trend was found in the variations with respect to time. Possible reasons for this variation are the deviating stability of the scanner and the phantom composition. No degradation of metabolites was found.

When performing consecutive measurements in ten healthy control subjects, the CV ranged from 1.99% for NAA to 8.23% for Cho, indicating an inherent signal variation of the system. For Cho, this was somewhat higher than for the other metabolites, which can be attributed to underlying J-coupling evolutions and small metabolic fluctuations [39,52]. So far, all variation could be attributed to variation in the methodological setup, which includes the influence of spectral noise, data analysis, repositioning of the subject, the phantom and voxel volume. Signal variation was also verified in a longitudinal experiment in which a male healthy volunteer was followed up during one year with CVs smaller than 5% for NAA and tCr and smaller than 10% for Ins. Again, signal variation for Cho was the highest ($\pm$12%). Intra-subject variation was similar to that reported in the literature [53]. Inter-subject variation varied from approximately 10% for NAA and tCr to approximately 20% for Cho and Ins, which were values that were somewhat higher than in a previous report [53]. Next to the methodological variation described above, there is also the inherent biological variation, which can be further complicated by pathology.

In both phantoms and human subjects, following shimming, the FWHM of the metabolites was always less than 12 Hz except in the case of the in vivo water resonance ($\pm$15 Hz). The somewhat higher, yet acceptable linewidth of the water resonance is probably due to the central occipital localization of the voxel with a high contribution of CSF, affecting the B_0 homogeneity. The VOI (8 ml) was placed in the primary visual cortex close to the skull and the subcutaneous fat, all contributing to susceptibility issues and B_0 inhomogeneities. Phantom experiments demonstrated the importance of shimming and B_0 homogeneity.

Table 5 The different errors on the absolute metabolite concentrations (of the 25 control subjects) when the correction factors were not taken into account, using the phantom replacement technique

	$[c_i]$ (mmol/(kg ww), ±SD)	CV of error on absolute metabolite concentration (%, ±SD)						
	All corrections	No c_{T2}	No c_{T1}	No c_{csf}	No c_{load}	No c_{temp}	No corrections	Int. wat.[a]
NAA	11.39 ± 1.35	−11.55 ± 2.14	14.49				−33.05 ± 6.07	1.5
tCr	8.96 ± 1.37	−18.16 ± 3.86	12.34	−11.06	−21.44	−5.48	−39.24 ± 5.84	0.8
Cho	1.58 ± 0.47	−19.22 ± 8.78	13.95	±3.15	±5.28		−39.17 ± 8.49	2.5
Ins	2.46 ± 0.65	–	24.20				−16.53 ± 5.41	2.4

[a] The CV is based on the average differences in concentration between both quantification methods, as seen in Table 4

The water signal intensity did not show significant variation with respect to the VOI position. The spatial uniformity has important implications for quantification methods involving external standards. Signal variation at greater distances from the coils isocenter is of relevance to techniques in which an external reference is placed adjacent to the head of the subject. The results shown in Fig. 7 indicate signal intensity variations of 4.47% on average. Large signal variations can be caused by standing radiofrequency waves [36]. Standing waves can be compensated by using a small and/or doped water phantom [36,54,55], as used in our study. Signal variations were quite similar between different NaCl-doped phantoms and with the smallest signal variation in the 1%NaCl-doped phantom which corresponded to the physiological NaCl concentration. Highest variation was found closest to the edge of the phantoms, because of susceptibility artifacts. Other contributions to signal variations are related to eddy currents and coil loading, as well as the intrinsic inhomogeneity of the B_1 field of the RF coil. Most variation was found away from the isocenter. These coil-dependent signal variations are present in in vivo and phantom measurements. The external calibration method used in this study relies on the ratio of the in vivo signal and the phantom signal obtained at the same location with respect to the coil and given the small signal variation in the center of the coil, it is expected that the error caused by these coil-related variations will be minimal. Separate optimization of the excitation pulse angle at each VOI location had little effect on the signal profile, and this alone is not a satisfactory approach to the problem of spatial variation in signal intensity.

Correction factors

A first correction was applied for T_1 and T_2 relaxation effects. The T_2-values were measured in all subjects separately and also compensated individually. Except for the T_2-value of Cho, all in vivo values corresponded well with literature values [52,56]. The T_2-values of Cho (i.e. 148 ± 38 ms) in this study were significantly lower than in previous reports [52, 56]. A potential reason for this could be the interference with underlying J-coupled resonances which are dependent on the echo time [52]. Due to T_2-decay, the signal was reduced by 1.7% in the phantom and 18.6% in vivo, indicating a correction for T_2-relaxation was only needed for the in vivo data. The inter-subject variation for the T_2 of NAA, tCr and Cho was approximately 12, 16 and 26%, respectively, indicating a substantial biological variation, especially for Cho and Ins. When using an average T_2-value or a literature value, the error in the quantified concentration might have been as high as 0.13 mmol/(kg wet weight) in the case of Cho, which is not negligible. For resonances of coupled spin systems such as Ins, J-modulation strongly affects both the signal intensity and the spectral lineshape and hence, complicating the determination of reproducible T_2-values. The signal of Ins does not follow a single- or double-exponential with multiple echo times, so the T_2-value of Ins could not be determined. There is a lack of literature values concerning the in vivo T_2 of Ins, and only a few studies report values varying from 110 to 279 ms in the occipital cortex; however, these values were obtained at a field strength of 1.5 T [57–59]. It also has to be emphasized that T_2 decreases with increasing field strength. So taking all this into consideration, absolute Ins concentration was not corrected for T_2 in vivo, resulting in an error on the actual concentration. This would explain the discrepancy in absolute Ins concentration between this study and previous studies [39]. When not correcting for T_2, the error on the concentration could amount to 19.22%, as was the case for Cho (Table 5; Fig. 8).

In vivo T_1 relaxation times were also measured, although in a separate group of age- and gender-matched subjects. These values were similar to literature values [52,56]. A relatively short TR (i.e. 2,000 ms) was used in the experiments, so T_1 correction was necessary since the tCr signal was reduced to 64.6% in the phantom and 75% in vivo because of incomplete longitudinal magnetization recovery. The inter-subject variation for the T_1-value of NAA, tCr, Cho and Ins was approximately 7, 10, 17 and 18%, respectively, indicating a substantial biological variation for Cho and Ins. There were no significant differences in relaxation times between MwoA patients and controls. Both T_1 and T_2 relaxation times of NAA, tCr, Cho, Ins and water were also measured in a phantom. These values can be used for relaxation time corrections

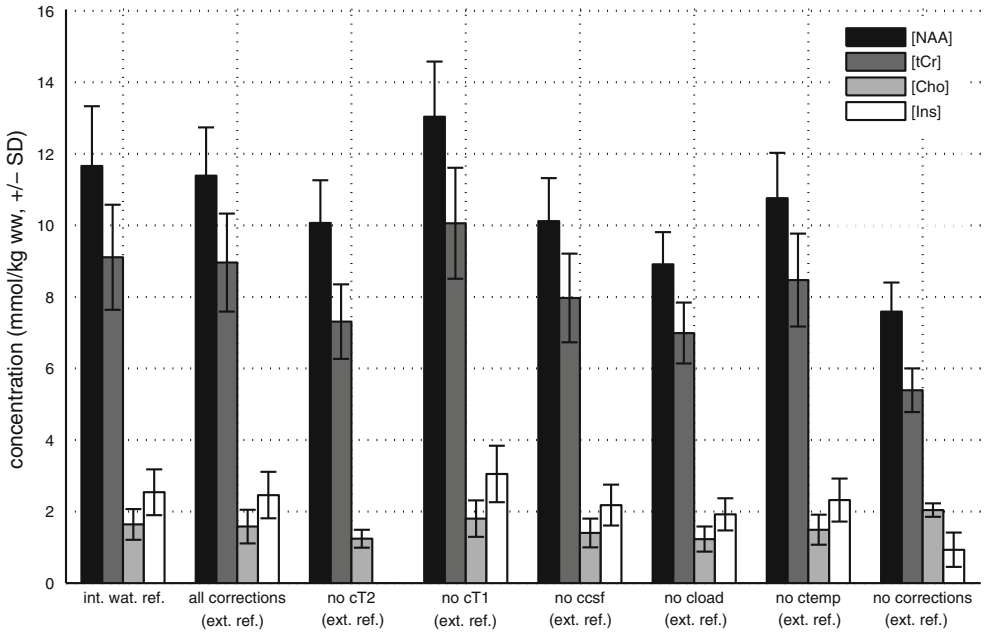

Fig. 8 Absolute metabolite concentrations (mmol/(kg wet weight) ±SD) when the different correction factors are not applied, using the phantom replacement technique (ext. ref.). The bars on the extreme left illustrate the absolute metabolite concentrations, obtained with the internal water reference (int. wat. ref.)

when using an external reference standard. In contrast to the in vivo values, phantom T_2-values are much higher. When not correcting for T_1, the error on the concentration could amount to 24.20%, as was the case for Ins (Table 5; Fig. 8).

The partial volume effect of CSF is derived by fitting a double-exponential function to the water-unsuppressed signal as a function of TE. On average, the CSF content was 11.84% and thus had a significant effect on the ultimate metabolite concentrations (Table 5; Fig. 8). When not accounted for, this would have led to an underestimation of the metabolite concentrations. This high contribution of CSF was due to the central occipital localization of the voxel and was in accordance with CSF values in a previous study in the same brain region [56]. No significant differences were found between MwoA patients and controls. When not using a correction for the partial volume effect, the error in the quantified concentration might have been as high as 1.32 mmol/(kg wet weight) in the case of NAA.

A fourth correction was made for the different coil loading between the phantom and the in vivo measurement. Coil loading has a large influence on the final absolute concentration values when comparing with an external reference phantom. When not correcting for coil loading, the error on the concentration was 21.44% (Table 5; Fig. 8).

The fifth and final correction factor concerned the temperature difference between the human subjects and the external reference phantom. Since no significant variations were observed over the phantom measurements, a constant correction factor of approximately 5% was attributed to all in vivo measurements. When not correcting for temperature, the error on the concentration was 5.48% (Table 5; Fig. 8).

Patients vs controls

In this work, we performed absolute quantification of proton metabolites in the occipital visual cortex of 22 MwoA patients and 25 control subjects. Effects of signal relaxation, CSF contribution, coil loading and temperature difference between the external reference phantom and in vivo were compensated for.

No significant differences in absolute metabolite concentrations nor in metabolite ratios were found between MwoA patients and controls. This confirms the earlier results of Sarchielli et al., although they did not perform a quantitative ^{1}H-MRS study [21]. We did not observe a decreased NAA or increased Lac concentration as seen in several studies, performed in MwA [19–21]. Sarchielli et al. observed a decrease in NAA (even before visual stimulation) in MwA patients [21]. More specifically, NAA is considered a neuronal marker, synthesized and located prevalently in neuronal mitochondria, and it is assumed to be involved in mitochondrial/cytosolic carbon transport [60]. In migraine patients, both MwA and MwoA, a disturbance of the interictal energy metabolism has been demonstrated [10–16] and the finding of a NAA decrease in MwA patients would, according to Sarchielli et al., indicate a less efficient mitochondrial

functioning in MwA patients compared to MwoA patients and controls [21]. This decrease in occipital NAA could not be confirmed by another study in which no significant differences were found between FHM patients, a rare type of MwA, and controls [20].

In addition, when using the internal water reference, the absolute values were very similar to the concentrations obtained with the phantom replacement technique. We can therefore conclude that both methods, with their own specific inherent difficulties, lead to comparable data (Table 5; Fig. 8).

Limitations

In this study, we did not consider the quantification of other metabolites such as Lac and Glx.

Because of both the chemical shift displacement artifact and anomalous J-modulation at 3 T and using a PRESS sequence, the Lac resonance showed a reduced or absent signal intensity at an echo time of 144 ms [61], which can lead to a severe underestimation of Lac. The extent of the signal loss due to anomalous J-modulation can vary considerably depending on the field strength, the used coil and the sequence parameters. A recommendation is to acquire also a spectrum at an echo time of 288 ms but the Lac peak, however, was only detected in a few subjects, including both patients and controls. A possible reason could have been the decreased sensitivity due to T_2 relaxation at longer echo times. Strategies to reduce the signal loss due to anomalous J-modulation usually requires changes in the sequence programming.

Glx signal strengths were also processed, but due to the unreliable quantification in unedited spectra, the values were not included in this study. We did, however, perform an initial AMARES analysis of Glx and did not observe any differences between MwoA patients and controls (data not shown). Since the partial overlap of NAA and Glx resonances can interfere with the NAA quantification at low TE and in the presence of possible Glx changes between MwoA patients and controls, a similar analysis was performed at longer TE [62]. Still no differences were observed between MwoA patients and controls. A possible solution to exclude these ambiguities in the future is to use the QUEST algorithm, as demonstrated in a previous study [63].

Conclusion

In this study, absolute quantification with ^{1}H-MRS was performed in an experimental migraine study in a homogeneous patient group. To obtain reliable absolute concentrations, however, several methodological aspects were investigated in depth and compensated for. Absolute quantification showed no differences in metabolite concentrations in the occipital visual cortex between MwoA patients and controls, in contrast to results obtained by relative quantification in earlier studies. When no corrections were applied for relaxation times, CSF, temperature and coil loading, absolute concentration errors could amount to approximately 40%, emphasizing the importance of these correction factors.

Acknowledgments This research is funded by the Special Research Fund PhD-grant B/07768/02 and performed at GIfMI. The Department of Radiotherapy is also greatly acknowledged for the use of the Radiophysics lab.

References

1. Lance JW, Goadsby PJ (1998) Mechanism and management of headache. Butterworth-Heinemann, Boston
2. Silberstein SD, Lipton RB, Goadsby PJ (1998). In: Goadsby PJ (ed) Headache in clinical practice, edn. Isis Medical Media, Oxford, pp 69–112
3. Olesen J, Tfelt-Hansen P, Welch KMA (2000) The headaches. Williams & Wilkins, Philadelphia
4. The International Headache Society Classification Subcommittee (2004) The international classification of headache disorders. 2. Cephalalgia 24(S1):1–160
5. Stovner LJ, Zwart JA, Hagen K, Terwindt GM, Pascual J (2006) Epidemiology of headache in Europe. Eur J Neurol 13(4):333–345
6. Edmeads J, Mackell JA (2002) The economic impact of migraine: an analysis of direct and indirect costs. Headache 42(6):501–509
7. Leonardi M, Steiner TJ, Scher AT, Lipton RB (2005) The global burden of migraine: measuring disability in headache disorders with WHOs classification of functioning, disability and health (ICF). J Headache Pain 6(6):429–440
8. Schoenen J (1994) Pathogenesis of migraine: the biobehavioural and hypoxia theories reconciled. Acta Neurol Belg 94(2):79–86
9. Schoenen J (1998) Cortical electrophysiology in migraine and possible pathogenic implications. Clin Neurosci 5(1):10–17
10. Welch KM, Levine SR, D'Andrea G, Helpern JA (1988) Brain pH in migraine: an in vivo phosphorus-31 magnetic resonance spectroscopy study. Cephalalgia 8(4):273–277
11. Welch KM, Levine SR, D'Andrea G, Schultz LR, Helpern JA (1989) Preliminary observations on brain energy metabolism in migraine studied by in vivo phosphorus 31 NMR spectroscopy. Neurology 39(4):538–541
12. Barbiroli B, Montagna P, Cortelli P, Martinelli P, Sacquegna T, Zaniol P, Lugaresi E (1990) Complicated migraine studied by phosphorus magnetic resonance spectroscopy. Cephalalgia 10(5):263–272
13. Sacquegna T, Lodi R, De Carolis P, Tinuper P, Cortelli P, Zaniol P, Funicello R, Montagna P, Barbiroli B (1992) Brain energy metabolism studied by 31P-MR spectroscopy in a case of migraine with prolonged aura. Acta Neurol Scand 86(4):376–380
14. Barbiroli B, Montagna P, Cortelli P, Funicello R, Iotti S, Monari L, Pierangeli G, Zaniol P, Lugaresi E (1992) Abnormal brain and energy metabolism shown by 31P magnetic resonance spectroscopy in patients affected by migraine with aura. Neurology 42(6):1209–1214
15. Montagna P, Cortelli P, Monari L, Pierangeli G, Parchi P, Lodi R, Iotti S, Frassineti C, Zaniol P, Lugaresi E, Barbiroli B (1994) 31P-Magnetic resonance spectroscopy in migraine without aura. Neurology 44(4):666–669
16. Uncini A, Lodi R, Di Muzio A, Silvestri G, Servidei S, Lugaresi A, Iotti S, Zaniol P, Barbiroli B (1995) Abnormal brain

and muscle energy metabolism shown by 31P-MRS in familial hemiplegic migraine. J Neurol Sci 129(2):214–222
17. Lodi R, Montagna P, Soriani S, Iotti S, Arnaldi C, Cortelli P, Pierangeli G, Patuelli A, Zaniol P, Barbiroli B (1997) Deficit of brain and skeletal muscle bioenergetics and low brain magnesium in juvenile migraine: an in vivo 31P magnetic resonance spectroscopy interictal study. Pediatr Res 42(6):866–871
18. Boska MD, Welch KM, Barker PB, Nelson JA, Schultz L (2002) Contrasts in cortical magnesium, phospholipid and energy metabolism between migraine syndromes. Neurology 58(8):1227–1233
19. Watanabe H, Kuwabara T, Ohkubo M, Tsuji S, Yuasa T (1996) Elevation of cerebral lactate detected by localized 1H-magnetic resonance spectroscopy in migraine during the interictal period. Neurology 47(4):1093–1095
20. Sandor PS, Dydak U, Schoenen J, Kollias SS, Hess K, Boesiger P, Agosti RM (2005) MR-spectroscopic imaging during visual stimulation in subgroups of migraine with aura. Cephalalgia 25(7): 507–518
21. Sarchielli P, Tarducci R, Preciutti O, Gobbi G, Pelliccioli GP, Stipa G, Alberti A, Capocchi G (2005) Functional 1H-MRS findings in migraine patients with and without aura assessed interictally. Neuroimage 24(4):1025–1031
22. Dichgans M, Herzog J, Freilinger T, Wilke M, Auer DP (2005) 1H-MRS alterations in the cerebellum of patients with familal hemiplegic migraine type 1. Neurology 64(4):608–613
23. Jacob A, Mahavish K, Bowden A, Smith ET, Enevoldson P, White RP (2006) Imaging abnormalities in sporadic hemiplegic migraine on conventional MRI, diffusion and perfusion MRI and MRS. Cephalalgia 26(8):1004–1009
24. Schulz UG, Blamire AM, Corkill RG, Davies P, Styles P, Rothwell PM (2007) Association between cortical metabolite levels and clinical manifestations of migrainous aura: an MR-spectroscopy study. Brain 130(Pt12):3102–3110
25. Gu T, Ma XX, Xu YH, Xiu JJ, Li CF (2008) Metabolite concentration ratios in thalami of patients with migraine and trigeminal neuralgia measured with 1H-MRS. Neurol Res 30(3):229–233
26. Macri MA, Garreffa G, Giove F, Ambrosini A, Guardati M, Pierelli F, Schoenen J, Colonnese C, Maraviglia B (2003) Cerebellar metabolite alterations detected in vivo by proton MR spectroscopy. Magn Reson Imaging 21(10):1201–1206
27. Ma Z, Wang SJ, Li CF, Ma XX, Gu T (2008) Increased metabolite concentration in migraine rat model by proton MR spectroscopy in vivo and ex vivo. Neurol Sci 29(5):337–342
28. Grimaldi D, Tonon C, Cevoli S, Pierangeli G, Malucelli E, Rizzo G, Soriani S, Montagna P, Barbiroli B, Lodi R, Cortelli P (2010) Clinical and neuroimaging evidence of interictal cerebellar dysfunction in FHM2. Cephalalgia 30(5):552–559
29. Naressi A, Couturier C, Castang I, de Beer R, Graveron-Demilly D (2001) Java-based graphical user interface for MRUI, a software package for quantitation of in vivo/medical magnetic resonance spectroscopy signals. Comput Biol Med 31(4):269–286
30. Laudadio T, Mastronardi N, Vanhamme L, Van Hecke P, Van Huffel S (2002) Improved Lanczos algorithms for blackbox MRS data quantitation. J Magn Reson 157(2):292–297
31. Vanhamme L, van den Boogaart A, Van Huffel S (1997) Improved method for accurate and efficient quantification of MRS data with use of prior knowledge. J Magn Reson 129(1):35–43
32. Cavassila S, van Ormondt D, Graveron-Demilly D (2001) Cramer-rao bound analysis of spectroscopic signal processing methods. In: Yan H (ed) Signal processing for magnetic resonance imaging and spectroscopy, edn. Marcel Dekker, New York, pp 613–640
33. Tofts PS (2004) Spectroscopy: 1H metabolite concentrations. In: Tofts P (ed) Quantitative MRI of the brain: measuring changes caused by disease. John Wiley, Chichester, pp 299–340
34. Drost DJ, Riddle WD, Clarke GDAAPM MR Task Group #9 (2002) Proton magnetic resonance spectroscopy in the brain: report of AAPM MR Task Group #9. Med Phys 29(9):2177–2197
35. Kreis R (2004) Issues of spectral quality in clinical 1H magnetic resonance spectroscopy and a gallery of artifacts. NMR Biomed 17(6):361–381
36. Tofts PS (1994) Standing waves in uniform water phantoms. J Magn Reson B 104(2):143–147
37. Insko EK, Bolinger L (1993) Mapping of the rafiofrequency field. J Magn Reson A 103(1):82–85
38. Helms G (2008) The principles of quantification applied to in vivo proton MR spectroscopy. Eur J Radiol 67(2):218–229
39. Kreis R (1997) Quantitative localized 1H MR spectroscopy for clinical use. Prog Nucl Mag Res Sp 31:155–195
40. Hennig J, Pfister H, Ernst T, Ott D (1992) Direct absolute quantification of metabolites in the human brain with in vivo localized proton spectroscopy. NMR Biomed 5(4):193–199
41. Soher BJ, van Zijl PC, Duyn JH, Barker PB (1996) Quantitative proton MR spectroscopic imaging of the human brain. Magn Reson Med 35(3):356–363
42. Helms G (2000) A precise and user-independent quantification technique for regional comparison of single volume proton MR spectroscopy of the human brain. NMR Biomed 13(7):398–406
43. Hoult DI, Richards RE (1976) The signal-to-noise ratio of the nuclear magnetic resonance experiment. J Magn Reson 24(1): 71–85
44. Ernst T, Kreis R, Ross BD (1993) Absolute quantitation of water and metabolites in the human brain. I. Compartments and water. J Magn Reson B 102(1):1–8
45. Lynch J, Peeling J, Auty A, Sutherland GR (1993) Nuclear magnetic resonance study of cerebrospinal fluid from patients with multiple sclerosis. Can J Neurol Sci 20(3):194–198
46. Hetherington HP, Pan JW, Mason GF, Adams D, Vaughn MJ, Twieg DB, Pohost GM (1996) Quantitative 1H spectroscopic imaging of human brain at 4.1 T using image segmentation. Magn Reson Med 36(1):21–29
47. Helms G (2003) T2-based segmentation of periventricular paragraph sign volumes for quantification of proton magnetic paragraph sign resonance spectra of multiple sclerosis lesions. Magn Reson Mater Phy 16(1):10–16
48. Connelly A, Jackson GD, Duncan JS, King MD, Gadian DG (2004) Magnetic resonance spectroscopy in temporal lobe epilepsy. Neurology 44(8):1411–1417
49. Lundbom N, Gaily E, Vuori K, Paetau R, Liukkonen E, Rajapakse JC, Valanne L, Hakkinen AM, Granstrom ML (2001) Proton spectroscopic imaging shows abnormalities in glial and neuronal cell pools in frontal lobe epilepsy. Epilepsia 42(12):1507–1514
50. Mathews VP, Barker PB, Blackband SJ, Chatham JC, Bryan RN (1995) Cerebral metabolites in patients with acute and subacute strokes: concentrations determined by quantitative proton MR spectroscopy. AJR Am J Roentgenol 165(3):633–638
51. Chang L, Ernst T, Tornatore C, Aronow H, Melchor R, Walot I, Singer E, Conford M (2001) Metabolite abnormalities in progressive multifocal leukoencephalopathy by proton magnetic resonance spectroscopy. Neurology 48(4):836–845
52. Mlynarik V, Gruber S, Moser E (2001) Proton T1 and T2 relaxation times of human brain metabolites at 3 Tesla. NMR Biomed 14(5):325–331
53. Schirmer T, Auer DP (2000) On the reliability of quantitative clinical magnetic resonance spectroscopy of the human brain. NMR Biomed 13(1):28–36
54. Ozdemir MS, Reyngoudt H, De Deene Y, Sazak HS, Fieremans E, Delputte S, D'Asseler Y, Derave W, Lemahieu I, Achten E (2007) Absolute quantification of carnosine in human calf muscle by proton magnetic resonance spectroscopy. Phys Med Biol 52(23):6781–6794

55. Keevil SF, Barbiroli B, Brooks JC, Cady EB, Canese R, Carlier P, Collins DJ, Gilligan P, Gobbi G, Hennig J, Kugel H, Leach MO, Metzler D, Mlynarik V, Moser E, Newbold MC, Payne GS, Ring P, Roberts JN, Rowland IJ, Thiel T, Tkac I, Topp S, Wittsack HJ, Wylezinska M, Zaniol P, Henriksen O, Podo F (1998) Absolute metabolite quantification by in vivo NMR spectroscopy: II. A multicentre trial of protocols for in vivo localised proton studies of human brain. Magn Reson Imaging 16(9):1093–1106
56. Ethofer T, Mader I, Seeger U, Helms G, Erb M, Grodd W, Ludolph A, Klose U (2003) Comparison of longitudinal metabolite relaxation times in different regions of the human brain at 1.5 and 3 Tesla. Magn Reson Med 50(6):1296–1301
57. Frahm J, Bruhn H, Gyngell ML, Merboldt KD, Hanicke W, Sauter R (1989) Localized proton NMR spectroscopy in different regions of the humanbrain in vivo. Relaxation times and concentrations of cerebral metabolites. Magn Reson Med 11(1):47–63
58. Kreis R, Fusch C, Maloca P, Felbinger J, Boesch C (1994) Supposed pathology may be individuality: interindividual and regional differences of brain metabolite concentration determined by 1H MRS. In Proceedings of 2nd meeting of the society of magnetic resonance. San Francisco, USA, 45pp
59. Kreis R, Ernst T, Ross BD (1993) Absolute quantitation of water and metabolites in the human brain. II. Metabolite concentrations. J Magn Reson B 102(1):9–19
60. Clark JB (1998) N-acetyl aspartate: a marker forn neuronal loss or mitochondrial dysfunction. Dev Neurosci 20(4–5):271–276
61. Lange T, Dydak U, Roberts TP, Rowley HA, Bjeljac M, Boesiger P (2006) Pitfalls in lactate measurements at 3T. AJNR Am J Neuroradiol 27(4):895–901
62. Clementi V, Tonon C, Lodi R, Malucelli E, Barbiroli B, Iotti S (2005) Assessment of glutamate and glutamine contribution to in vivo N-acetylaspartate quantification in human brain by 1H-magnetic resonance spectroscopy. Magn Reson Med 54(6):1333–1339
63. Malucelli E, Manners DN, Testa C, Tonon C, Lodi R, Barbiroli B, Iotti S (2009) Pitfalls and advantages of different strategies for the absolute quantification of N-acetylaspartate, creatine and choline in white and grey matter by 1H-MRS. NMR Biomed 22(10):1003–1013